Recycling of Superbase-Based Ionic Liquid Solvents for the Production of Textile-Grade Regenerated Cellulose Fibers in the Lyocell Process

Elsayed, Sherif

2020-09-21

Elsayed , S , Helminen , J , Hellsten , S , Guizani , C , Witos , J , Rissanen , M , Rantamäki , A H , Hyväri , P , Varis , P , Wiedmer , S K , Kilpeläinen , I & Sixta , H 2020 , ' Recycling of Superbase-Based Ionic Liquid Solvents for the Production of Textile-Grade Regenerated Cellulose Fibers in the Lyocell Process ' , ACS Sustainable Chemistry & Engineering , vol. 8 , no. 37 , pp. 14217-14227 . https://doi.org/10.1021/acssuschemeng.0c05330

http://hdl.handle.net/10138/333626
https://doi.org/10.1021/acssuschemeng.0c05330

unspecified
acceptedVersion

ARTICLE

Recycling of Superbase-Based Ionic Liquid Solvents for the Production of Textile-Grade Regenerated Cellulose Fibres in the Lyocell Process

Received 00th January 20xx,
Accepted 00th January 20xx

DOI: 10.1039/x0xx00000x

S. Elsayed,[a] S. Hellsten,[a] C. Guizani,[a] J. Witos,[a] M. Rissanen,[a] A. H. Rantamäki,[b] P. Varis,[c] S. K. Wiedmer[b] and H. Sixta *[a]

Ioncell® is a Lyocell-based technology for production of man-made cellulose fibres. This technology exploits the intrinsic dissolution power of superbase-based ionic liquids (ILs) towards cellulose. The regenerated fibres are produced via a dry-jet wet spinning process, in which the cellulose filaments are stretched in an air gap before regenerating in an aqueous coagulation medium. In order to commercialize this process, it is essential to prove the techno-economic feasibility of this technology. That said, many important criteria are to be met, among them selecting a solvent with high cellulose dissolution power, proving a stable spinning process and yielding fibres of good mechanical properties. Most of all, it is critical to demonstrate the recovery of the solvent from the coagulation bath without impairing its solvation power. This study reports on the spinnability and recyclability of the IL 7-methyl-1,5,7-triazabicyclo[4.4.0] dec-5-enium acetate ([mTBDH][OAc]) over five cycles in comparison to 1,5-diaza-bicyclo[4.3.0]non-5-enium acetate ([DBNH][OAc]). The ILs were recovered from the coagulation bath by consecutive thermal treatments under reduced pressure. Accordingly, the recovered ILs were utilized to dissolve 13 wt.% cellulose in each cycle, without the addition of make-up IL, to form a homogeneous solution suitable for the dry-jet wet spinning. Using [mTBDH] [OAc], cellulose could be fully dissolved in all five cycles. In contrast, cellulose dissolution was only possible with fresh [DBNH][OAc] as the ability to dissolve cellulose was lost after the first recovery. This study focuses on the composition of the recovered ILs and the extent of side-products generation. Additionally, we present the rheological properties of the solutions as well as the macromolecular and mechanical properties of the regenerated fibres. Also, the toxicity of both solvents was investigated using Vibrio fischeri bacteria. Finally, the spun fibres from all [mTBDH][OAc] spinning trials were combined to produce a demonstration dress (Paju), designed and sewn by Marimekko Design House in Finland.

Introduction

The reliance of the textile industry on cotton to meet the growing market demand has been declining since the early 2000s.[1] The increase in the demand for textile fibres is not only due to the growth in global population but also due to the change in consumer behaviour. To fill the gap, the need of petroleum-based fibres, mainly polyester, has steadily increased to contribute to a total market share of 62% in 2018 compared to 26% for cotton and only 6% for wood-based fibres.[2]

Ioncell® is an air gap spinning technology for the production of man-made cellulose fibres for textile and technical applications. This Lyocell-based technology exploits the capabilities of protic superbase-based (ILs) to directly dissolve cellulose without the need of derivatization. The dissolution occurs via disrupting the hydrogen bond system, triggered by the anion of the IL that binds to the polar domains of cellulose, while the superbase cation interacts with the non-polar domains by Van der Waals interaction forces.[3,4] In this way, a homogeneous solution with a high cellulose concentration (13 – 17 wt.%) is readily formed.[3,5] Similar to the Lyocell technology, which is based on N-methylmorpholine N-oxide (NMMO), the dissolved cellulose filaments are stretched in an air gap before immersing in a water-containing coagulation bath, where cellulose regeneration takes place.[5,6] The phase transfer to the regenerated cellulose fibres occurs by the diffusion of the non-solvent (water) into the cellulose solution (dope) and the simultaneous diffusion of the solvent molecules into the coagulation bath, thus creating the regenerated structure.[7] Recently, evidence has been published that characterizes the first part of the regeneration as density fluctuations, most likely caused by spinodal decomposition.[8]

Over the course of the spinning process, the IL therefore accumulates in the coagulation bath. As soon as a certain concentration is reached, the spin bath solution must be fed to a

[a] Department of Bioproducts and Biosystems, Aalto University, P.O. Box 16300, FI-00076 Aalto, Finland. E-mail: sherif.elsayed@aalto.fi, sanna.hellsten@aalto.fi, chamseddine.guizani@aalto.fi, marja.rissanen@aalto.fi, herbert.sixta@aalto.fi
[b] Department of Chemistry, University of Helsinki, P.O. Box 55, FI-00014 University of Helsinki, Helsinki, Finland. E-mail: antti.rantamaki@helsinki.fi, susanne.wiedmer@helsinki.fi
[c] Marimekko Corporation, P.O. Box 107, Puusepänkatu 4, 00811 Helsinki, Finland. E-mail: pauliina.varis@marimekko.fi
† Footnotes relating to the title and/or authors should appear here.
Electronic Supplementary Information (ESI) available: [details of any supplementary information available should be included here]. See DOI: 10.1039/x0xx00000x

solvent recovery system together with the washing streams. In the recovery process, it is essential to remove enough water from the IL in order to maintain an efficient dissolution of cellulose in the following cycles. For lower cellulose concentrations of 7 – 8 wt.%, previous studies with similar ILs showed that it is required to achieve ≤ 4.1 wt.% of residual water for complete cellulose dissolution.[9,10]

The choice of an optimum recycling strategy is governed by the thermal stability of the IL and its interactions with water. Such interactions are based on the size and the structure of the IL as well as the hydrophilicity and the strength of the bond between the base and the conjugated acid.[11] Theoretically, several recycling strategies can be applied to recover ILs. Yet, not all of them are feasible to be adopted in the Ioncell® technology, since it is necessary to avoid drastic conditions (temperature and pressure) that can induce possible degradations in the solvent. This section briefly discusses the different recycling techniques and highlights the reasons in favour or against some of them. The adsorption separation method, typically applied using activated carbon, is favourable for hydrophobic systems, where the high selectivity of the sorbent is sufficient to adsorb one of the components. However, due to the hydrophilic nature of the selected ILs, a fraction of the water may also be adsorbed along with the IL, thus reducing the separation efficiency.[12] Additionally, heating is usually required in order to regenerate the sorbent, which may induce IL degradations. Another method is liquid-liquid extraction, which is more compatible for IL/organic systems. Dibble *et al.* reported a recovery of 89% for the separation of 1-ethyl-3-methylimidazolium acetate ([emim][OAc]) from pre-treated biomass by using a solvent mixture containing mainly acetone and isopropanol.[13] However, for the same reason, liquid-liquid extraction is not applicable to Ioncell® due to the high hydrophilicity of the solvent, and the fact that introducing a new component to the process may increase the complexity of the recycling. Besides, the reported recovery rate is considerably low and therefore, not economically and environmentally sustainable.

Evaporation is one of the more common ways to separate IL-water systems. The separation mechanism relies on the difference between the low vapour pressure of the ILs and the higher volatility of water. It is a simple method but requires a high energy input. As already employed in the NMMO-based Lyocell process, this method yields recovery rates > 99%.[14] Additionally, there are also several reports on high recoveries of ILs using evaporation.[9,15–17] As promising as it sounds, the high thermal exposure of the IL during the separation may initiate thermal decomposition and undesired side-products,[9,18] more on this issue regarding Ioncell® ILs is discussed in the next section. Similarly, IL-water solutions can be separated by pervaporation. Despite also delivering high recovery rates (~ 99%), this method requires low viscose solutions in combination with elevated temperature and prolonged treatments (100 °C and 5 hr), making it industrially unviable for superbase-based ILs.[19,20]

For purification purposes, crystallization is a convenient technique for separating solids and removing traces of water from the IL, while avoiding solvent losses.[21,22] Unfortunately, the sole reliance on crystallization to achieve full recovery of dilute IL solutions might not be feasible, since preliminary solid-liquid equilibrium studies reveal the need for extremely low temperatures, ca. - 75 °C, in order to obtain a coherent separation.[23]

When constructing the optimum recycling strategy for the Ioncell® solvent system, a combination of more than one separation method may be of higher benefit. For example, the combination of evaporation to preconcentrate the IL followed by crystallization, or a combined evaporation - pervaporation system. Despite the lower energy costs of some non-thermal water removal processes per process stage, the specific energy advantages of multi-effect evaporation processes, possibly in combination with vacuum, are significantly higher. For this reason, we select evaporation as the sole recycling route. This is to investigate the thermal stability of the ILs and to explore the effect of generated side-products on the state of the cellulose solution. Additionally, as mentioned above, this method has already proven its success in the recovery of NMMO. Hence, it is useful to establish a point of reference for the Ioncell® process.

1,5-diaza-bicyclo[4.3.0]non-5-enium acetate ([DBNH][OAc]) is an amidine-based superbase IL that has proven to be an excellent cellulose solvent. When synthesized in equimolar composition, cellulose of high concentrations (13 – 17 wt.%) is rapidly dissolved at mild temperatures (≤ 80 °C) in less than 90 min.[5,24,25] Possibly, this is correlated to the Kamlet-Taft solubility parameters (H-bond accepter, β, and H-bond donor, α) that describe the capabilities of direct solvents in general.[26,27] Parviainen *et al.* (2013) expressed that the net-basicity (β - α) as a function in β is a useful empirical function that characterize the potential of IL solvents towards cellulose. While adopting this function, it was confirmed that [DBNH][OAc] ((β - α) of 0.49 and β of 1.11), together with other guanidine- and imidazole-based ILs belong to the good category of cellulose solvents.[3] The physical and thermodynamic properties of [DBNH][OAc] are available in Ostonen *et al.* (2016) and Ahmad *et al.* (2016). Moreover, the cellulose solutions, prepared from [DBNH][OAc], exhibit adequate viscoelastic properties for producing high quality cellulose fibres through the dry-jet wet spinning technology.[5,25] Despite the previous, there has been concerns about the thermal stability of this IL during the recovery from the coagulation bath.[9]

During the recovery of equimolar [DBNH][OAc] from the diluted aqueous solution by thermal treatment, the IL undergoes a hydrolysis reaction, producing undesirable side-products. The pathway of the hydrolysis initiates by the reaction of water (a nucleophile) with the unsaturated nitrogenous group of the amidine-based IL, producing 1-(3-aminopropyl)-2-pyrrolidone acetate ([APPH][OAc]).[9,28] While the hydrolysis reaction is reversible, under more drastic conditions an irreversible acetylation reaction of the primary amine to 1-(3-acetamidopropyl)-2-pyrrolidone (APPAc) may occur.[9] Consequently, the enrichment of such hydrolysis products in the solvent mixture leads to the impairment of the solvation capabilities of the IL, which jeopardises the economic feasibility of the Ioncell® process, since large make-up amounts of the solvent are required to compensate for the IL losses.

In addition, a recent study revealed that during the removal of water from a diluted [DBNH][OAc] solution, the IL tends to vaporize

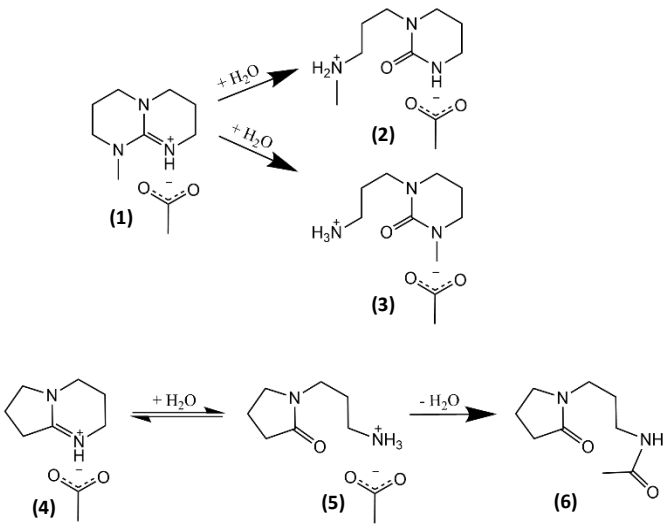

Figure 1. Hydrolysis of [mTBDH][OAc] (1) into [H-mTBD-1][OAc] (2) and [H-mTBD-2][OAc] (3) and hydrolysis of [DBNH][OAc] (4) into [APPH][OAc] (5) and condensation into APPAc (6)

with the water fraction in a non-equimolar ratio, leaving behind a concentrated IL solution with an acid-to-base molar ratio greater than 1. The mechanism of evaporation is described by the dissociation of the ionic compounds into neutral species, which in return are more prone to vaporization because of weak interaction forces among them.[29,30] It was found that DBN exhibits higher molar effusion rates than the acid during evaporation, despite the higher volatility of the latter. This is due to the ability of the de-ionized acid to form H-bonds with the ion pair in the condensed phase, therefore increasing the IL acid-to-base ratio.[30] Further increase in the temperature and duration of the thermal exposure is met by additional elevation in the solvent acid-to-base ratio, reaching an azeotropic composition of 5:3, at which the solvent is most thermally stable as noticed by exhibiting lowest vapour fraction.[28] On the other hand, neutral acetic acid is not a cellulose solvent, so the presence of excess acid in the solvent is unfavourable. For the IL recovery in Ioncell®, most of the water can be removed while avoiding such elevated acid-to-base ratios. Also, in the context of a closed-loop process, the distillate stream containing dilute IL solution (from vaporization) can be utilized as a first fibre-washing step and/or recycled back to the coagulation bath to avoid solvent losses.

As mentioned above, one can expect a deviation in the composition of the recovered IL when thermally recovered in the Ioncell® process. Herein, we define the main parameters influencing the properties of the recovered solvent as residual water, hydrolysis products and acid-to-base molar ratio. The concentration of these parameters in the recovered IL in a continuous close-loop operation, may have an impact on the dissolution behaviour of cellulose and, consequently, the quality of the spinning solution. As previously mentioned, other classes of superbases can be employed in the IL synthesis. Owing to their physical and thermal properties, these classes can demonstrate different tolerance towards hydrolysis and vaporization during the IL recovery, and therefore can be a viable alternative.

An interesting guanidine-based IL solvent is 7-methyl-1,5,7-triazabicyclo[4.4.0] dec-5-enium acetate ([mTBDH][OAc]). Like [DBNH][OAc], it lies in the category of good cellulose dissolving solvents, expressing higher (β - α) of 0.79 than [DBNH][OAc] that implies an improved solvation power.[31] mTBD is also susceptible to hydrolysis reactions yielding a mixture of the hydrolysed base (H-mTBD), comprised of 1-[3-(methylammonio)propyl]-1,3-diazinan-2-onemium acetate (H-mTBD-1) and 1-(3-ammoniopropyl)-3-methyl-1,3-diazinan-2-onemium acetate (H-mTBD-2).[32] In a quantitative comparison between the hydrolysis of mTBD and DBN in water, Hyde et al (2019) reported that 32% of DBN but only 3.4% of mTBD was hydrolysed at 27 ºC after 4 hours. The improved hydrolytic stability shown by mTBD is associated with the higher electron density at the sp^2-hybridized carbon of guanidines than amidines, which relatively protects them against nucleophilic reactions.[32] For this reason, one may expect less hydrolysis products when using the guanidine-based IL as a solvent in Ioncell®, which should have a positive effect on the specific solvent requirements. *Figure 1* shows the generated hydrolysis products of [DBNH][OAc] and [mTBDH][OAc] ILs.

In this study, we investigate the use of [mTBDH][OAc] as a cellulose solvent in Ioncell® process in five recovery cycles. Utilizing a batch set-up, the IL was employed to dissolve 13 wt.% of cellulose and produce regenerated cellulose fibres. The highly water-diluted IL present in the coagulation bath was concentrated by successive thermal treatments and thus recovered. The study presents the rheological properties of the cellulose solution as well as the macromolecular and mechanical properties of the regenerated cellulose fibres produced in each cycle. Concurrently, [DBNH][OAc] was also subjected to the same cellulose spinning and recovery process for a single cycle. The compositions of the two superbase-based ILs, [mTBDH][OAc] and [DBNH][OAc], after recovery are compared in terms of residual water content, IL concentration, extent of hydrolysis products and acid-to-base molar ratio. Furthermore, we report the toxicity of both solvents. Finally, to demonstrate the quality and the potential of the regenerated fibres from the fresh and recycled [mTBDH][OAc], a demonstration dress was produced by Marimekko PLC.

Experimental

Materials

Equimolar [DBNH][OAc] was prepared in Aalto University by the addition of glacial acetic acid (100%, Merck, Darmstadt, Germany) to DBN (99% Fluorochem, Hadfield, UK) in a monitored temperature reaction that was set not to exceed 70 °C under continuous stirring for 1 hour. [mTBDH][OAc] was synthesized at the University of Helsinki by the addition of, likewise, equimolar acetic acid to mTBD, while continuously stirring in a controlled temperature reaction.[3] The prepared IL was received in the form of solid crystals and used as such. Cellulose of birch prehydrolysis kraft pulp (Enocell) (Pure by Stora Enso, Enocell mill, Uimaharju, Finland, intrinsic viscosity of 494 ml/g) was received in the form of pulp sheets and ground in a Wiley mill.

Cellulose dissolution and spinning

Before pulp addition, the freshly synthesized [mTBDH][OAc] was melted inside a vertical kneader at a temperature of 85 °C for 2 hours. Similarly, the fresh [DBNH][OAc] was liquefied in a water bath at 80 °C for 2 hours. The recovered [mTBDH][OAc] and recovered [DBNH][OAc] were melted in a water bath at 80 °C for 1 hour. Next, the liquid ILs were transported to the vertical kneader for mixing with the cellulose.

After ensuring complete melting of the IL in every cycle, 13 wt.% of cellulose (based on the total mass of the cellulose and the liquid fraction) was added to the IL and manually stirred for 1 min. The mixture was then let to stir (30 RPM, 75 min and 15 mbar) at a temperature of 85 and 80 °C for the [mTBDH][OAc] and [DBNH][OAc], respectively. Shortly after, the dissolved cellulose solution was filtrated by the means of a hydraulic press filtration system (150 bar, metal filter fleece, 5 – 6 µm absolute fineness). The clear solution was then shaped to a final form adequate for the dimensions of the spinning cylinder and stored.

On the spinning day, the dope was first fed into the spinning cylinder and pre-heated at 85 °C for 2 hours. Spinning took place using a customized dry-jet wet piston spinning unit (Fourné Polymertechnik, Germany). For the spinning process, the extruded dope filaments were stretched in an air gap and regenerated in a 110 – 125 L water coagulation bath with a fixed controlled temperature of 12 °C before being collected on a spinning godet. The employed spinneret had the dimensions of 200 holes, 100 µm diameter and a length-to-diameter ratio of 0.2. The air gap distance was fixed to 1 cm and the godet take-up velocity was 12 times higher than that of the 3.5 m/min extrusion velocity, *i.e.* the exerted draw ratio (DR) was 12. During spinning, the dope temperature was controlled at 83 – 87 °C for the dopes containing [mTBDH][OAc] and 78 – 82 °C for the dope containing [DBNH][OAc]. Shortly after spinning, the regenerated cellulose filaments were collected and cut into 4 cm long pieces. Thereafter, they were washed to rinse-off the residual IL. The washing procedure was conducted in a batch process at 80 °C for 2 hours. The spent washing water was changed to fresh at half-time.

Light microscopy, molar mass distribution and dope rheology characterization

The state of cellulose dissolution was observed directly after dope preparation using Axio Zeiss A1 optical light microscope equipped with a polarizer. The microscope was set to cross-polarized mode and the images were analysed for the total dissolution content via ImageJ v1.52t software.

Molar mass distribution (MMD) was determined (for the pulp and the obtained fibres from every cycle) using gel permeation chromatography system with Dionex Ultimate 3000 HPLC module. The set-up of the system consisted of four analytical columns (4 x Agilent PLgel Mixed-A. 7.5 x 300 mm), a refractive index detector (Shodex RI-101), Viscotek/Malvern SEC/MALS 20 multi-angle light-scattering detector and a precolumn (PLgel Mixed-A, 7.5 x 50 mm). Lithium chloride/*N,N*-dimethylacetamide was used as a solvent. Preparation of the samples followed a sequence of cellulose activation via solvent exchange process, as described in a previous protocol.[33] The detector constants for refractive index and multi-angle light scattering were determined using a narrow polystyrene standard (Mw = 96 000 g/mol, Đ = 1.04) dissolved in 0.9% LiCl in *N,N*-dimethylacetamide. Checking for the detector calibration was achieved using a broad polystyrene standard (Mw = 248 000 g/mol, Đ = 1.73). The ∂n/∂c value of 0.136 mL/g was used for celluloses in 0.9% LiCl in *N,N*-dimethylacetamide.[34]

Utilizing the smoothening feature in Origin 2019b software (Loess method with a span of 0.1), we were able to remove the noise from the acquired MMD peaks. From the smoothened data, it was easy to calculate the necessary values of the degree of polymerization (DP), number average molar mass (M_n) and weight average molar mass (M_w).

Dope samples were run for shear rheological properties using an Anton Paar MCR 302 rheometer (25 mm plate diameter, 1 mm gap size). The measuring sequence employed an oscillatory test over a temperature range of 70 – 100 °C in steps of 10 °C. The chosen angular frequencies, ω, were 0.01 – 100 s^{-1} with a constant shear rate of 1%. For this sequence, the complex viscosity, η*, the storage moduli, G', and the loss moduli, G'', were recorded. The zero-shear viscosity, η0, was determined for every temperature point by fitting the data to Cross viscosity model, given by the below equation, where C and p are (cross) time and rate constant, respectively. The cross-over point (COP) is the point of intersection of both loss and storage moduli and an important indication for the elasticity of the dope under certain conditions.

$$\eta = \frac{\eta_0 - \eta_\infty}{1 + (C\dot{\gamma})^p} + \eta_\infty$$

Fibre measurements and birefringence

Fibres breaking tenacity, elongation at break, linear density and breaking force were measured on an automatic single-fibre tensile tester (Favigraph, Textechno, Germany) for conditioned and wet measurements. The test implemented a gauge length of 20 mm, testing speed of 20 mm/min and a specimen number of 20. The maximum load of the cell was 20 cN. The fibres were pretensioned with a 100 mg weight throughout the test. During the wet state test, the fibre with the pretension weight was mounted to the upper clamp and the fibre was immersed into deionized water for 10 seconds before the tensile testing. Following this, the lower clamp was closed, and the specimen remained immersed during the whole test.

The fibres total orientation was characterized by a polarized light microscope (Zeiss Axio Scope) equipped with a 5λ Bereck compensator. The birefringence, Δn, was calculated by dividing the retardation of the polarized light by the fibre diameter. The total orientation, f_t, was then determined by dividing Δn by the maximum birefringence of cellulose (0.062).[35]

Recycling of the solvent

The coagulation bath solution was filtrated prior to recycling with filter paper (VWR) of 12 – 15 µm particle retention cut-off at room temperature. The recovery of [mTBD][OAc] took place through a set of thermal treatment operations. First, the dilute coagulation bath was fed into a centrifuge evaporator (Alfa Laval Centritherm) at 62 °C, 250 mbar absolute, 400 rpm and a feed flow rate of 50 kg/hr. The distillate stream containing only traces of IL was disposed and not recycled back. Meanwhile, the residue stream containing a higher concentrated IL was further concentrated in a two consecutive evaporation stages using an agitated thin-film evaporator (UIC GmbH, RF10). In both steps, a pump feed rate of 3.5 kg/hr was used. The applied conditions in the 1st stage were as follows, residue temperature of 61 °C, pressure of 20 mbar absolute and agitation speed of 400 rpm. In the 2nd stage, the residue temperature was 82 °C, vacuum pressure of 17 mbar and the same agitation speed as in the 1st stage.

The concentrated residue stream (recovered IL) of the 2nd stage of the thin-film evaporation was recycled back to the kneader to prepare the dope for the following cycle without any addition of make-up IL. Following the evaporator, a condenser set at 2 °C was fixed to fully condense the evaporated lighter fraction (distillate). Likewise, the two distillate streams from the condenser of the 1st and the 2nd stage of the thin-film evaporator were recycled to the coagulation bath of the following cycle. A general overview of the adopted process including dissolution, fibre spinning, and IL recycling is presented in *Scheme 1*. The recycling of [DBNH][OAc] followed the same scheme under the same conditions with the exception of a lower temperature (75 °C) used in the 2nd stage thin-film evaporator.

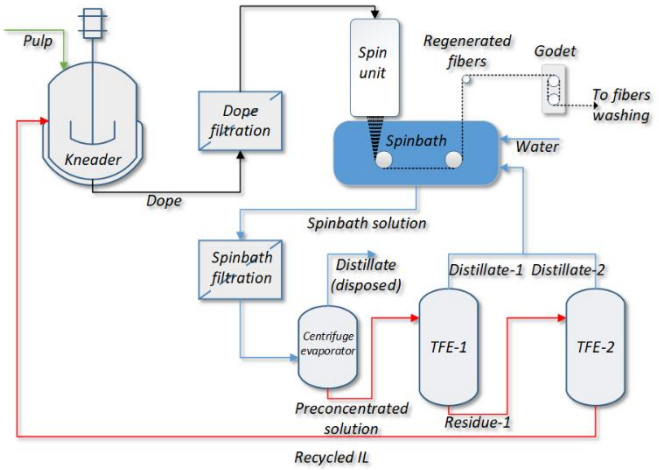

Scheme 1. General overview of the process showing cellulose dissolution, spinning of regenerated fibres and recycling of the diluted IL

Analysis of IL-containing streams

Concentrate streams

The composition of the concentrate streams from both stages of the thin-film evaporators was characterized by proton nuclear magnetic resonance (^{1}H NMR) spectroscopy with dimethyl sulfoxide (DMSO-d6) (Sigma-Aldrich, purity > 99.9%) as a solvent. The spectra of the samples were acquired at 23 °C using a Bruker 400 MHz Ultra Shield NMR instrument with eight transients and an acquisition time of 2.5 s. The peaks chemical shifts and integral values were identified by the aid of MestReNova software.

The water content of the recovered ILs from the 2nd stage of the thin-film evaporator was determined by Karl Fischer titration equipped with a DL38 volumetric Karl Fischer Titrator (Mettler Toledo) using Hydranal Methanol Rapid as a solvent and Hydranal Composite 5 as a titrant (Fluka Analytical).

Distillate streams

The composition of dilute IL-containing streams was analysed using capillary electrophoresis (CE). The analysis of mTBD, DBN, and their hydrolysis products were carried out with an Agilent 7100 CE system from Agilent Technologies (Santa Clara, CA, USA) equipped with a diode-array detector and an air-cooling device for the capillary cassette. Baird *et al.* (2019) have reported the capillary coating and analysis methodology previously. In brief, the calibration curves were acquired for mTBD, DBN, and their degradation products at a concentration range of 0.01 mg·mL^{-1} to 0.2 mg·mL^{-1}. Benzyltrimethylammonium chloride (Sigma Aldrich, Steinheim, Germany) with 0.02 mg/mL concentration was used as an internal standard. The CE separation was as follows: voltage - 25 kV (mTBD and its degradation products), - 20 kV (DBN and its degradation products), sample injection 10 s at 10 mbar, temperature of the cassette and the autosampler 25 °C, and UV detection at 200 nm. The background electrolyte (BGE) solution was composed of sodium acetate buffer at pH 4.0 with the ionic strength of 10 mM and 20 mM for DBN and its decomposition products, and likewise, for mTBD and its decomposition products. The pH of the BGE solutions was adjusted to the desired value with 1M sodium hydroxide or 1 M hydrochloric acid. Before use, the BGE solution was filtered through a 0.45 µm PVDF filters (Phenomenex, Denmark).

The acetate concentration was determined following a modified capillary zone electrophoresis method.[36,37] The CE experiments were performed with a Hewlett Packard ^{3D}CE model G1600GX (Agilent, Waldbronn, Germany). The acetate calibration curve was comprised of nine acetic acid solutions with concentrations between 0.0025 mg/mL and 0.2 mg/mL. Propionic acid (Acrõs Organics/Thermo Fischer Scientific, Geel, Belgium) with a 0.05 mg/mL concentration was used as an internal standard. The correlation coefficient of the calibration curve was 0.9997. The BGE solution was composed of 20 mM 2,3-pyridinedicarboxylic acid (Sigma-Aldrich, Steinheim, Germany) and 0.3 mM myristyltrimethylammonium hydroxide (100 mM concentrate, Waters, Milford, USA) in 10:90 (v/v) MeOH:H_2O. The pH of the solution was adjusted to 9 with 25% (v/v) ammonia (VWR international, Leuven, Belgium). The buffer was filtered through a 0.45 µm PVDF filter (Aireka Cells, Wan Chai, Hong Kong) before use. The sample was injected hydrodynamically at 45 mbar for 10 s. The separation was performed using a voltage of - 10 kV at 25 °C and the indirect UV detection was done by a diode-array UV-Vis detector at 254 nm.

Toxicity assay

The toxicities of the compounds were established by measuring their median effective concentrations (EC_{50}) values using *Vibrio fischeri* bacteria and a Microtox luminometer/thermostate apparatus (Modern Water, USA). The choice of *Vibrio fischeri* bacteria is based on a study by Lechuga *et al.* to detect most sensitive bacteria for surface-active toxicants.[38] Even though this compound in this work cannot directly be classified as surface active, these bacteria were selected for the toxicity assessment of the compounds studied in this work. The response measured in the assay is the decay of bioluminescence produced by the bacteria itself. Briefly, the bioluminescence value was first measured before the exposure to the compounds. After this, the bacteria were exposed to at least four different compound concentrations in a 2% (w/v) NaCl solution, and the decay in the bioluminescence was recorded. The EC_{50} value was defined based on the concentration-dependent decay of the bioluminescence. The toxicities were defined at set time intervals of 5 and 15 minutes. Two independent measurements were done for each IL as duplicates.

Demonstration dress

The dress making process included spin finishing of the fibres and yarn spinning (Aalto University, Finland), weaving and fabric making (Söktaş Tekstil A.Ş, Turkey), printing and dress making (Marimekko Oy, Finland) and wear trials. The Ioncell® [mTBDH][OAc] fibres in the dress contributed to a total of 38% (weft) with the rest (warp) made from Tencel™ fibres. For a complete description of the process, please see supporting ESI, dress making.

Results and discussion

In order to recover the IL from the filtered coagulation bath, water as the lighter fraction was removed from the IL solution by evaporation. In a commercial plant, all washing solutions would also be included in the water evaporation process. However, before evaporation, impurities formed by degradation reactions of the solute in a closed-loop operation must be purified in a partial stream in such a way that they do not exceed a threshold concentration that would impair the spinning process. Due to the extremely low and undetectable concentration of impurities in a laboratory plant set-up, also the rather low temperatures for cellulose dissolution and fibre spinning, the removal of these substances is neither necessary nor possible and therefore not the subject of this work.

In a batch-scale Ioncell® process, the term 'number of cycles' is given to describe the stability and sustainability of the process. Typically, one cycle consists of cellulose dissolution and homogenization followed by fibre spinning and washing and finally the recovery of the solvent from the coagulation bath before the next cycle commences. Hence, it is a way to simulate the process for a continuous operation. The main draw-back of the batch set-up is the losses arising from the manual handling of the various steps, which will inevitably affect the stability of the closed-loop process; especially, when the process consists of sensitive procedures such as the fibre spinning step. It is also important to mention that no solvent make-up was used in this study.

In a closed-loop operation, there is a risk that with an increasing number of cycles, the build-up of impurities and side-products in the solvent can negatively affect the quality and rheology of the cellulose solution and thus the stability of the spinning process. Therefore, it is logical to first discuss the recovery process of the IL before correlating the solvent composition to the subsequent steps (dope preparation and fibre spinning). The main parameters influencing the properties of the recovered solvent are the amount of residual water, hydrolysis products, and the acid-to-base molar ratio of the IL.

Recycling of [mTBDH][OAc]

Over the five cycles, the amount of [mTBDH][OAc] used in the batch spinning process changed from the original 1.7 kg to only 0.25 kg during the fifth cycle due to handling losses. Accordingly, the concentration of the IL in the 120 L coagulation bath decreased from 1.4 to 0.2 wt.%. As shown in *Scheme 1*, due to the low [mTBDH][OAc] concentration, most of the water was first removed by a centrifugal evaporator before the preconcentrated IL solution was further concentrated in a two-stage thin-film evaporator (TFE-1 and TFE-2) to such an extent that it could be reused in the preparation of the cellulose dope. *Table 1* shows the residual water contents before and

Table 1. Residual water concentrations of [mTBDH][OAc] streams before and after the consecutive evaporator units measured by Karl-Fischer (KF) titration and capillary electrophoresis (CE).

Cycle	Before centrifuge evaporator*	Before TFE-1	Before TFE-2	Recovered IL
	wt.%	wt.%	wt.%	wt.%
Fresh IL				0.2 ± 0.01
1	98.5 ± 0.1	54.4 ± 1.2	15.1 ± 1.1	3.1 ± 0.1
2	98.8 ± 0.2	76.9 ± 0.5	14.3 ± 0.3	2.2 ± 0.05
3	99.2 ± 0.04	93.7 ± 0.4	29.2 ± 1.2	2.7 ± 0.05
4	99.7 ± 0.02	90.7 ± 0.4	26.6 ± 0.8	2.8 ± 0.02
5	99.9 ± 0.01	92.8 ± 0.6	57.6 ± 3.2	2.6 ± 0.04

* Values calculated indirectly by capillary electrophoresis (CE) as the difference between the total sample amount and the total amount of the measured compounds (base, acid and degradation products).

after the respective distillation stages. An old centrifugal evaporator was utilized for preconcentration, but due to many technical problems, the IL concentration after the centrifugal evaporator was generally low (especially in cycles 3 – 5) and with a large scatter. However, the large variation in the water content was well compensated by the two subsequent thin-film evaporators, so that the water content of the recovered IL (after TFE-2) was generally below 3 wt.% and showed only small variations from cycle to cycle (*Table*). Thus, despite technical shortcomings, the water content in the recycled IL could be adjusted very precisely. On the other hand, due to the high volume of the distillate from the centrifugal evaporator, the distillate was not recycled to the spin bath and disposed instead. The distillate streams from TFE-1 and TFE-2 were mixed and pumped back to the spin bath of the following cycle.

Generally, during the thermal recovery of the superbase-IL (accompanied with vacuum), minor fractions of the IL vaporize in a non-equimolar ratio with the water to the distillate stream.[30] Also, the IL can undergo a hydrolysis reaction with water producing an undesirable side-product, illustrated in *Figure 1*, which may act as a non-solvent in the process.[9,28] The consumption of the IL in the hydrolysis reaction combined with its vaporization during the recovery leads to an increase in the acid-to-mTBD ratio in the recovered IL.

Table S2 in the ESI provides the composition of the concentrate and distillate streams in the centrifuge evaporator and TFE-1. The amount of hydrolysis products (H-mTBD) in the distillate and concentrate from the centrifuge evaporator were well below the detection limit, probably due to the mild conditions of the centrifugal bath (62 °C and 250 mbar) and the high IL dilution in the feed and the concentrate. For the same reasons, very little traces of hydrolysis products (< 0.06 wt.%) were detected in the distillate of TFE-1 (61 °C and 20 mbar) with no presence in the concentrate.

The final step of water removal in TFE-2 required the use of elevated conditions (82 °C and 17 mbar) to reach the desired low water contents. *Table* summarizes the composition of the concentrate and the distillate streams during the recovery of [mTBDH][OAc] in TFE-2 (final step) over the five cycles. The table provide the composition of the IL (content and acid-to-mTBD ratio), hydrolysis products and residual water in both streams. In the recovered solvent, [mTBDH][OAc] contributed to 94.5 – 96.8 wt.% of the total content. The composition of the recovered IL was analysed by NMR, displayed in *Figure 2,* where the integral of the methyl protons of the acetate and the base showed an increase in the acid-to-mTBD molar ratio from the equimolar fresh [mTBDH][OAc] to 1.1 – 1.16 in the recovered [mTBDH][OAc] (*Table 2*). Additionally, we detected minor hydrolysis products (0.5 – 2.6 wt.%) with the chemical shifts of H-mTBD-1 and H-mTBD-2 akin to the shift values reported in Hyde *et al.* (2019) at 2.24 and 2.78 ppm respectively. However, the magnitude of H-mTBD-2 was significantly lower than H-mTBD-1, suggesting a favoured yield of H-mTBD-1 resulting from the hydrolysis reactions.

The residual water content in the recovered IL was 2.6 – 3.1 wt.%, which is significantly below the limit value for the solubility of cellulose in [mTBDH][OAc]. A water content of ≤ 7.5 wt.% in the IL can be tolerated for complete dissolution of the cellulose, provided the acid-to-mTBD molar ratio is close to 1 and the amount of total hydrolysis products, H-mTBD, is insignificant.[39] Obtaining such a low residual water content is essential for the IL recovery, as water does not only induce hydrolysis products, but may also hinder cellulose dissolution and disrupt the viscoelastic properties of the dope. Regarding the distillate stream, a low content of the IL was present in the condensate with an average value of 0.7 wt.% (based on the evaporator feed IL) and a considerable low acid-to-mTBD molar ratio (0.06 – 0.24).

From the above results, despite the slight increase of the acid-to-mTBD ratio in the recycled IL and the minor conversion of the superbase into its hydrolysis products, we observed no real trend in the accumulation of the side-products over the five cycles. This suggests that an equilibrium composition between the superbase and the amine is reached, at the specified evaporation conditions, allowing the full recovery of the solvent mixture without further change in its composition. The reason for the enrichment of the

Table 2 Fresh [mTBDH][OAc] composition and the composition of the concentrate and distillate streams in the TFE-2 during recycling

Cycle	Concentrate stream				Distillate stream			
	[mTBDH][OAc]		H-mTBD	Water	[mTBDH][OAc]			H-mTBD
	wt.%	Acid-to-mTBD	wt.%	wt.%	wt.% of feed IL	±	Acid-to-mTBD	wt.% of feed IL
Fresh IL	99.8	0.99	-	0.2 ± 0.0	-	-	-	-
1	96.4	1.10	0.5	3.1 ± 0.1	1.5	0.03	0.06	0.37 ± 0.01
2	96.8	1.10	1.0	2.2 ± 0.1	0.9	0.03	0.11	0.27 ± 0.01
3	95.8	1.11	1.5	2.7 ± 0.1	0.6	0.03	0.07	0.16 ± 0.02
4	94.5	1.16	2.6	2.8 ± 0.0	0.2	0.02	0.24	0.98 ± 0.14
5	94.9	1.14	2.5	2.6 ± 0.0	0.3	0.07	0.15	0.18 ± 0.01
Avg	**95.7**	**1.12**	**1.6**	**2.7 ± 0.1**	**0.7**	**0.04**	**0.13**	**0.4 ± 0.04**

recovered IL with the acid component can be attributed to tendency of the neutral acid to form H-bonds with the ion pair in the liquid phase, while the neutral base is prone to vaporization.[30] The higher volatility of the base is also shown in the substantially low acid-to-mTBD ratio of the distillate(s).

acid-to-DBN molar ratio of 1.27. The distillate stream comprised 1.2 wt.% IL, 2.1 wt.% APPH, while no APPAc was detected in the trials.

Comparison of the recovery of the solvents

The extent of ILs vaporization has been previously linked to the fraction of neutral compounds present in the equilibrium mixture.

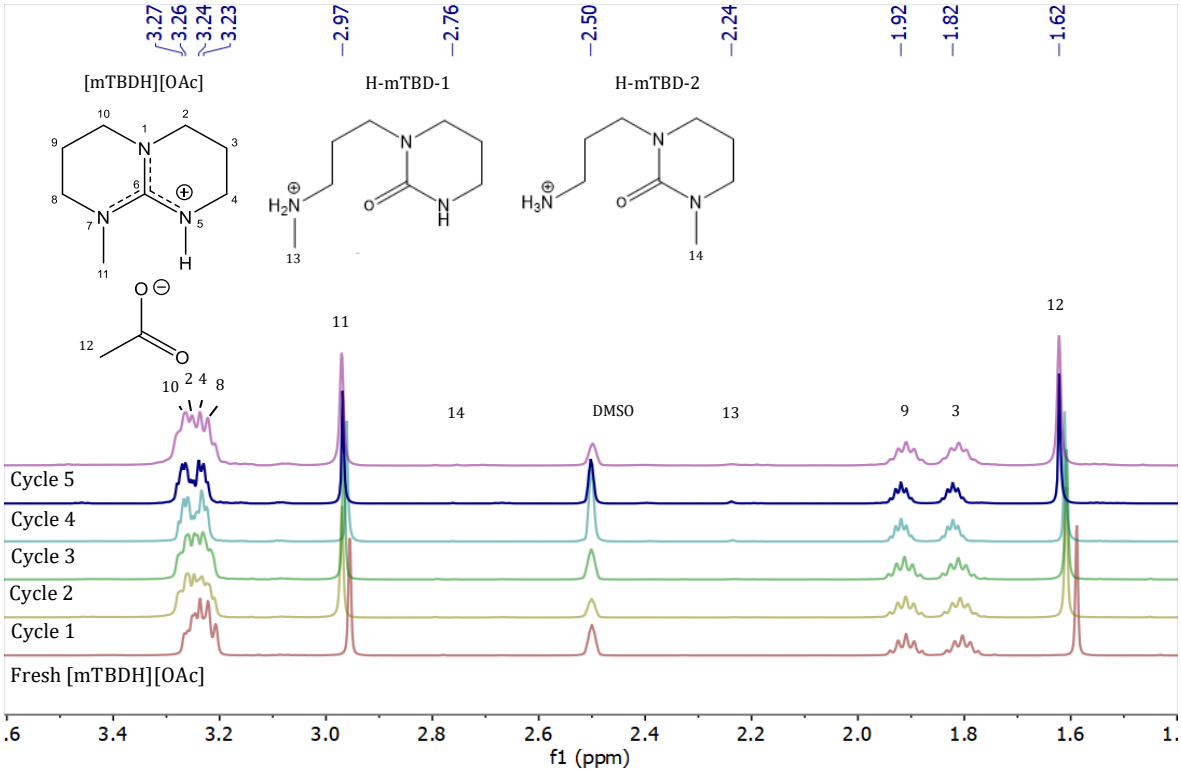

Figure 2. Stacked 1H NMR of fresh and recovered [mTBDH][OAc] IL showing the peaks of the acetate, the base and the hydrolysis products.

Recycling of the [DBNH][OAc]

The recycling of [DBNH][OAc] from the dilute spin bath solution was akin to [mTBDH][OAc] and followed the same sequence (centrifuge evaporator, TFE-1 and TFE-2). The only exception was the lower thin-film temperature applied in the last evaporation step, TFE-2 (75 °C), due to the higher vapor pressure of [DBNH][OAc] than [mTBDH][OAc]. *Table* reveals the composition of the concentrate and the distillate streams in TFE-2 while recovering [DBNH][OAc]. The table shows, already after one cycle, a significant amount of hydrolysis product (APPH) (14.4 wt.%) as well as 3.3 wt.% of residual water in the recovered [DBNH][OAc]. The content of the recovered IL was undoubtedly low at 86.4 wt.%, combined with an elevated

Typically, ionic compounds express strong cohesive forces that characterize them with low volatility, while the main fraction prone to vaporization is the neutral species due to weaker interactions.[30,40] The evaporation mechanism was described by several articles to start by the de-ionization of the ionic compounds followed by vaporization of the neutral species.[29,30] From literature, it can be assumed that the fraction of the neutral compounds in the equilibrium mixture for [DBNH][OAc] is greater than for [mTBDH][OAc]. This is because mTBD is a stronger base than DBN, pK_a 25.4 and 23.4, respectively (measured in acetonitrile solvent), therefore when conjugated with acid, a larger extent of ionicity is expected from [mTBDH][OAc].[41,42] Similarly, a relatively higher

Table 3 Fresh [DBNH][OAc] composition and the composition of the concentrate and distillate streams in TFE-2 during recycling

Cycle	Concentrate stream				Distillate stream		
	[DBNH][OAc]		APPH	Water	[DBNH][OAc]		APPH
	wt.%	Acid-to-base molar ratio	wt.%	wt.%	wt.% of feed IL	±	wt.% of feed IL
Fresh IL	99.8	0.99	-	0.1 ± 0.0	-	-	-
1	86.4	1.27	14.4	3.3 ± 0.1	1.2	0.3	2.1 ± 0.1

energy is needed in order to de-ionize the ionic compounds of [mTBDH][OAc]. From the previous reasons, it is obvious that the guanidine-based IL is thermally more stable than [DBNH][OAc]. This is reflected in the lower acid-to-base molar ratio (avg. 1.12) of the recovered [mTBDH][OAc] compared to 1.27 for the recovered [DBNH][OAc], and in the combined IL and hydrolysis fractions of 1.1 and 3.3 wt.% in the distillate stream for [mTBDH][OAc] and [DBNH][OAc], respectively.

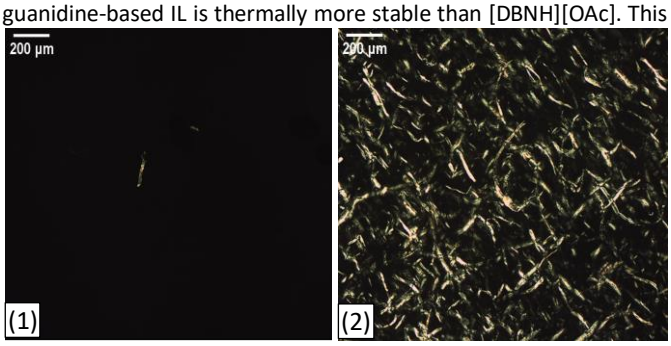

Figure 3. Dissolution of 13 wt cellulose using recovered [mTBDH][OAc] IL after the 5th cycle (1). Undissolved 13 wt.% cellulose using recovered [DBNH][OAc] IL (after the 1st cycle) (2).

Likewise, the improved hydrolytic stability of [mTBDH][OAc] is clearly visible in the significantly reduced hydrolysis products than [DBNH][OAc] (avg. 1.6 vs. 14.4 wt.%). This is in good alignment with the trend reported by Hyde et al. (2019), where it was shown that the higher electron density of the sp^2-hybridized carbon creates higher resistance against nucleophilic reactions in the guanidine-based superbases than the amidine-based superbases. Regarding cellulose dissolution, the combination of the side-products in the recovered [mTBDH][OAc] were well below the limitation threshold, which allowed full dissolution of 13 wt.% cellulose in all cycles. A dissolution limitation can be expected when the combination of the side-products is greater than the specified concentrations: 5.5 wt.% water, 1.2 acid-to-mTBD and 15 wt.% hydrolysis products.[39] On the other hand, cellulose dissolution was halted using the once recovered [DBNH][OAc] and could not proceed to a second cycle. Hence, the use of [DBNH][OAc] came to an end in these trials. *Figure 4* shows the full dissolution state (99.9 %) of the prepared dope using the recovered [mTBDH][OAc] in the 5th cycle, in contrast to only 76.5 % using the recovered [DBNH][OAc] from a single recovery cycle.

Although, previous studies reported the successful dissolution of 7 – 8 wt.% cellulose using recovered [DBNH][OAc] in the presence of comparable APPH concentrations.[9,43] The high cellulose content used in the Ioncell® process (13 wt.%) may justify the need of lower side-products in the [DBNH][OAc] after recovery; lower APPH, acid-to-DBN ratio and water contents than the values obtained here.

Solvents toxicity

When discussing the hydrolytic and thermal stabilities of both solvents, one should not overlook their toxicity. Many ILs are being labelled as green solvents with harmless effects on both humans and the environment. This is an important criterion, especially when promoting superbase-based ILs for cellulose dissolution as an alternative to the viscose process with all its negative environmental impacts. For the fresh solvents ([mTBDH][OAc] and [DBNH][OAc]) and their hydrolysis products (H-mTBD and APPH), the toxicity values are shown in *Table* . The values are expressed as both mg/L and mM, since both values are commonly used in the literature. Following the toxicity range used in a previous study,[44] namely that compounds are classified as harmless (EC_{50} values > 1 000 mg/L), practically harmless (100 – 1000 mg/L), moderately toxicity (10 – 100 mg/L), toxic (1 – 10 mg/L) or highly toxic (< 1 mg/L), we can see that all studied compounds can be classified as harmless (values in the range of 1548 – 8322 mg/L after 5 min exposure). Typically, longer exposure time (here 15 min) result in lower values (i.e. higher toxicity), and this was also the case for almost all compounds. The amide formations for both ILs were also tested, the results can be viewed in the ESI, Table S3. Since the compositions of the recovered solvents is a combination of water, IL and hydrolysis products, therefore it is valid to assume that their toxicity is also within the harmless region.

Cellulose dissolution and regeneration

The rheological properties of the fresh [DBNH][OAc] dope was discussed in previous studies,[5,6] in which it was revealed that the complex viscosity of the dope displays a Newtonian plateau at lower angular frequencies (< 0.001 s^{-1}) followed by a shear-thinning behaviour at higher frequencies (> 0.01 s^{-1}). In the latter phase, the dope possesses viscoelastic properties, expressed as COP, adequate for stretching and spinning. The COPs are the intersections of the loss moduli and storage moduli and express the viscous and elastic characteristics of the dope, respectively. Typically, in Ioncell® using [DBNH][OAc], a spinning window is optimal at zero-shear viscosities of 25 000 – 35 000 Pa.s and COPs ~ 4000 Pa, which usually

Table 4 EC_{50} values of the studied compounds using Vibrio fischeri bacteria

Compound	*Vibrio fischeri*			
	5 min		15 min	
	mg/L	mM	mg/L	mM
[DBNH][OAc]	4678 ± 609	25.4 ± 3.3	3257 ± 299	17.7 ± 1.6
APPH	8322 ± 69	41.1 ± 0.3	7704 ± 115	38.1 ± 1.0
[mTBDH][OAc]	1548 ± 128	7.3 ± 0.6	1173 ± 51	5.5 ± 0.2
H-mTBD	3402 ± 129	14.7 ± 0.6	3334 ± 37	14.4 ± 0.2

corresponds to angular frequencies around 1 s^{-1} and spinning temperatures of 75 – 80 °C.[5,25]

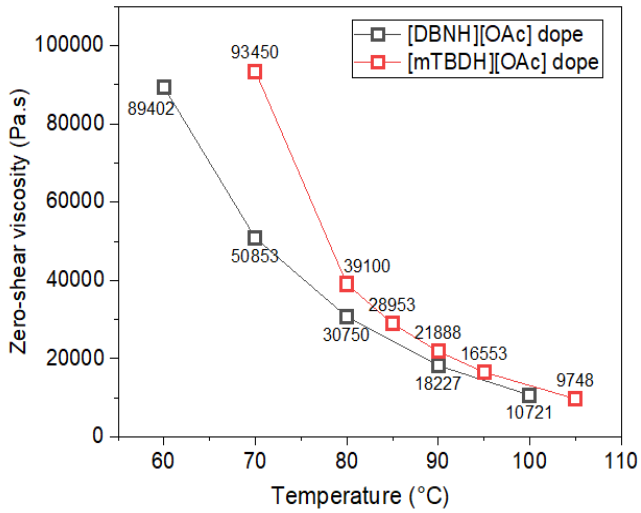

Figure 4 Zero-shear viscosity of fresh [mTBDH][OAc]dope vs fresh [DBNH][OAc] dope.

The fresh [mTBDH][OAc] dope exhibited a similar viscoelastic behaviour as fresh [DBNH][OAc] dope. The dope complex viscosity also showed a Newtonian plateau followed by a shear-thinning phase at higher angular frequencies. However, *Figure 4* indicates that the [mTBDH][OAc] dope displays a greater zero-shear complex viscosity than the [DBNH][OAc] dope (ca. 39 000 vs 30 000 at 80 °C respectively), suggesting a slightly higher spinning temperature for the former. This is due to the bigger viscosity associated with the mTBD superbase.[3] Furthermore, the [mTBDH][OAc] dope displayed COP that matched well with the spinning window discussed in Sixta *et al.* (2015). As for the recovered [mTBDH][OAc] dopes, the rheological properties were similar to those of the fresh one with only minor variations as illustrated in *Table* , implying no change in the IL - cellulose interactions from the presence of side-products.

For the fibre regeneration process, the spinning window was selected according to a zero-shear viscosity of 30 000 Pa·s with a tolerance of ± 2 °C and a COP modulus of around 4000 Pa, resulting in a spinning temperature range of 83 – 87 °C for the [mTBDH][OAc] dopes and of 78 – 82 °C for the fresh [DBNH][OAc] dope. Successful fibre spinning was achieved for the dopes of fresh as well as for the recovered [mTBDH][OAc] dopes. Contrarily, fibre spinning was only possible using the fresh [DBNH][OAc] dope, but not for the recovered [DBNH][OAc] dope since, as shown in *Figure 3*, the altered composition of the recovered IL hindered cellulose dissolution. The extruded filaments were pre-drawn in the spinneret holes before total orientation of the polymer chains took place in the air gap. Thereafter, the filaments immersed into a coagulating water medium, where desolvation and formation of regenerated cellulose filaments of high fibril structure density occurred.[7,45] Meanwhile, a DR of 12 was applied on the filaments by the spinning godet, to which they were collected.

Table and *Figure 5. Molar mass distribution of the Enocell pulp and the fibres obtained from the five cycles using [mTBDH][OAc] IL* present the MMD (Mn, Mw, DP > 2000 and 100 > DP) of the spun fibres in reference to the birch PHK pulp. The results revealed a minor degradation in the high and the low molecular weight fractions, DP > 2000 and 100 > DP, of cellulose fibres spun from the recovered [mTBDH][OAc] dopes. The slight decrease is noticed in DP > 2000 to values of 11.9 – 10.6 % and in DP < 100 to values of 4.4 – 4 % from 12.2 and 4.8 % in the original pulp, respectively. Fibres from fresh [mTBDH][OAc] dope, however, almost exhibited no change in

Table 5 Rheological properties of fresh and recycled dopes prepared from [mTBDH][OAc] and birch PHK pulp at a concentration of 13 wt.% at 85°C.

Cycle	Temperature °C	Complex viscosity η_0^* [Pa.s]	Angular frequency ω at COP [s^{-1}]	Complex modulus G'=G'' at COP [Pa]
1 (Fresh)	85	28 953	0.78	3 776
2	85	28 500	0.84	3 996
3	85	31 200	0.74	3 918
4	85	26 835	0.81	3 630
5	85	32 890	0.76	4 203
Avg.	**85**	**29 676**	**0.79**	**3 905**
Stdev	0	± 2 379	± 0.04	± 218

Table 6 Molar mass distribution of the pulp and the fibres obtained from the five cycles using [mTBDH][OAc]

	Enocell	Cycle 1	Cycle 2	Cycle 3	Cycle 4	Cycle 5
Mn, kDa	44.49	49.30	48.23	47.25	54.53	47.62
Mw, kDa	160.49	158.42	148.19	138.39	146.39	147.98
DP > 2000, %	12.2	12.6	11.9	10.6	11.5	11.6
DP < 100, %	4.8	4.4	4.4	4.6	4.1	4.0

cellulose molar mass distribution. The same behaviour is depicted with Mw. The relatively preserved MMD of cellulose fibres using recovered [mTBDH][OAc] indicates no severe degradation in the cellulose chains throughout the dissolution and spinning processes.

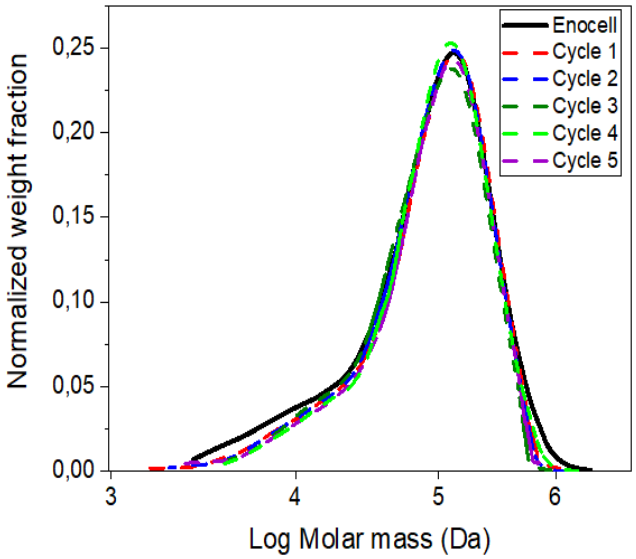

Figure 5. Molar mass distribution of the Enocell pulp and the fibres obtained from the five cycles using [mTBDH][OAc] IL

Table summarizes the important tensile properties and total orientation of the regenerated fibres of [mTBDH][OAc] in comparison to [DBNH][OAc] at 12 DR. All regenerated fibres exhibited a linear density of 1.2 – 1.3 dtex. Fibres of cycles 1, 2 and 3 expressed good tenacities that were similar to the that of the fibres produced from fresh [DBNH][OAc]. The shown tenacities are comparable to or higher than those of NMMO Lyocell-based fibres, which fits well within the textile application purposes.[46] Similarly, all fibres demonstrated a high wet-to-dry tenacity close to 1. This is an intrinsic feature of Lyocell fibres, where the high total orientation seems to preserve the fibres strength under wet state. On the other hand, the elongation at break for [mTBDH][OAc]-based fibres was lower than that of the [DBNH][OAc]-based fibres. The difference can be described by the influence of the different ILs on the restructuring of the cellulose chains, crystalline and amorphous regions, during the regeneration phase.[45]

Fibres spun in cycles 4 and 5, however, showed both lower tenacities and lower elongation at break than the fibres of the earlier cycles. One possible explanation could be the instability during the spinning arising from the small dopes and the short spinning time in the corresponding cycles. This is due to the handling losses of the IL in the different steps over consecutive cycles, yielding a recovered [mTBDH][OAc] amount in the 4th and 5th cycle only sufficient to prepare small dopes of 500 and 250 g, respectively. When taking into consideration the volume of the Fourné spinning unit (2.5 L) and the applied extrusion velocity, the duration of the total spinning process was reduced to less than 20 min for the 4th cycle and 10 min for the 5th cycle. Previously, it was observed since the development of the Ioncell® spinning activity that the instability of the spinning process, fibre breakages and agglomerates formation, increases as the dope amount in the spin unit approaches its end. The same behaviour was noticed in the 4th and the 5th cycle, in which the spinning was less stable than the previous cycles. The combination of the high total orientation values and low tensile properties of these fibres suggests a stiffer fibre structure. Yet, as shown in the rheological properties and the MMD, there is no justification that this is caused by the recovered IL, but rather due to a mechanical shortcoming.

Demonstration dress

The collected fibres from the [mTBDH][OAc] spinning trials were combined to produce the Ioncell® yarn, which was then combined with Tencel™ yarn for the weaving process according to the instructions of Söktaş Tekstil A.Ş (Turkey) weaving mill. The incorporation of Tencel™ as warp yarn in the dress making, 62% of the total fibre content, was essential since Söktas Tekstil A.Ş is an industrial mill and requires rather large amount of fibres that were not possible to produce in a lab-scale capacity. The yarn yield of [mTBDH][OAc] Ioncell® fibres was 95% with a linear density similar to the Tencel™ yarn as demonstrated in **Virhe. Viitteen lähdettä ei löytynyt.**. The breaking force and the breaking tenacity of the Ioncell® yarn are higher than the Tencel™ yarn, implying a higher total chain orientation of the former fibres. Meanwhile, the standard deviation of Ioncell® yarn is somehow large, which means that the evenness of the yarn fibres is slightly less. This is due to the small-scale production

Table 7 Tensile fibre conditioned properties from [mTBDH][OAc] (cycles 1-5) and [DBNH][OAc]

Fibres	Titer	Tenacity	Elongation	Total orientation	Wet-to-dry tenacity
	dtex	cN/tex	%	-	-
Cycle 1	1.2 ± 0.3	49.9 ± 3.8	9.5 ± 1.2	0.70 ± 0.06	0.99 ± 0.10
Cycle 2	1.3 ± 0.2	48.4 ± 2.8	9.3 ± 0.6	0.67 ± 0.06	0.99 ± 0.06
Cycle 3	1.2 ± 0.2	52.8 ± 3.2	10.1 ± 1	0.73 ± 0.11	0.97 ± 0.05
Cycle 4	1.3 ± 0.2	39.8 ± 4.6	7.5 ± 1.7	0.73 ± 0.04	1.01 ± 0.04
Cycle 5	1.2 ± 0.2	38.6 ± 3.3	8.5 ± 1.2	0.72 ± 0.07	1.01 ± 0.08
[DBNH][OAc]	1.2 ± 0.2	48.3 ± 2.8	13.7 ± 1.5	0.60 ± 0.11	0.97 ± 0.09

and the absence of auto-levelling possibility in the Ioncell® yarn production process. Table S1 in the ESI contains comprehensive

Table 1 Yarn mechanical properties for Marimekko demonstration dress

Yarn	Linear density	Breaking force	Elongation at break	Breaking tenacity
	tex	cN	%	cN/tex
[mTBDH][OAc]- Ioncell®	19.9 ± 0.9	490 ± 77	5.7 ± 0.7	24.6 ± 3.7
Tencel™	19.9 ± 0.2	443 ± 34	7.7 ± 0.7	22.3 ± 1.7

properties of the blended fabric.

The Paju dress designed by Marimekko, *Figure 6*, is featured with its unique navy-blue reactive dye (Huntsman Novacron® P). From the wearing trials of the dress, the fabric felt soft and nicely draped with a comfortable feeling to wear. When washed for the first time, the wet fabric was soft but upon drying, the fibres became slightly stiffer, and the interlining in the collar and cuffs started to slightly unfasten. After steam ironing, the fabric regained some of its softness. Wearing trials of the dress returned the softness to the fabric, which felt almost similar as prior to washing. Dimensional shrinkage was not observed after the washing. Even after the second and third wash, the results were similar to the first wash experience.

Figure 6 Marimekko's Paju dress. Designer: Riikka Buri, Marimekko. Photographer: Sebastian Johansson.

Conclusion

The presented results suggest that [mTBDH][OAc] is a harmless solvent that has a high ability to dissolve cellulose and thus can be used as a technically viable solvent in the Ioncell® process. Also, it was shown that [mTBDH][OAc] has a significantly higher thermal and hydrolytic stability during solvent recovery than [DBNH][OAc]. In this context, the results of the five cycles trial revealed that the combination of the side-products (residual water, hydrolysis products and different acid-to-base ratio) of the recovered [mTBDH][OAc] did not impair the dissolution of 13 wt.% cellulose. From this, we could assume that an equilibrium composition is established between the superbase and the amine during recovery, implying that the IL can be recovered almost completely with no additional degradations. On the other hand, the recovered [DBNH][OAc] lost its dissolution capability towards the same cellulose content already after the 1st cycle.

The rheological properties of the prepared dopes from the recovered [mTBDH][OAc] were akin to the fresh [mTBDH][OAc] dope, suggesting no change in the viscoelastic properties of the cellulose solution. Likewise, the preserved cellulose MMD, observed in fraction of DP > 2000 and M_w, indicates that the cellulose chains had no degradation during the dissolution by the recovered IL. The regenerated fibres from the first three cycles using [mTBDH][OAc] had good mechanical properties, however, fibres spun in cycles 4 and 5 showed inferior properties, probably due to limitations during the spinning process that led to mechanical shortcomings. Finally, the Paju dress designed by Marimekko demonstrates and highlights the good properties of the [mTBDH][OAc] Ioncell® yarn for the textile applications.

Conflicts of interest

There are no conflicts to declare.

Acknowledgements

This work was possible as a part of the Technical Development of Ioncell with special Emphasis on the Solvent Recycling (SolvRec) research program.

Notes and references

1 D. Eichinger, A vision of the world of cellulosic fibers in 2020, *Lenzinger Berichte*, 2012, **90**, 1–7.
2 *The Fiber Year. World survey on textiles & nonwovens*, 2019, http://www.thefiberyear.com/.
3 A. Parviainen, A. W. T. King, I. Mutikainen, M. Hummel, C. Selg, L. K. J. Hauru, H. Sixta and I. Kilpeläinen, Predicting cellulose solvating capabilities of acid-base conjugate ionic liquids, *ChemSusChem*, 2013, **6**, 2161–2169.
4 B. D. Rabideau, A. Agarwal and A. E. Ismail, The role of the cation

in the solvation of cellulose by imidazolium-based ionic liquids, *The Journal of Physical Chemistry B*, 2014, **118**, 1621–1629.
5 H. Sixta, A. Michud, L. Hauru, S. Asaadi, Y. Ma, A. W.T. King, I. Kilpeläinen and M. Hummel, Ioncell-F: A High-strength regenerated cellulose fibre, *Nordic pulp & paper research journal*, 2015, **30**, 43–57.
6 A. Michud, M. Hummel and H. Sixta, Influence of process parameters on the structure formation of man-made cellulosic fibers from ionic liquid solution, *J. Appl. Polym. Sci.*, 2016, **133**, 177.
7 H. A. Coulsey, The formation and structure of a new cellulosic fiber, *Lenzinger Berichte*, 1995, **75**, 60 (61).
8 Y. Nishiyama, S. Asaadi, P. Ahvenainen and H. Sixta, Water-induced crystallization and nano-scale spinodal decomposition of cellulose in NMMO and ionic liquid dope, *Cellulose*, 2019, **26**, 281–289.
9 A. Parviainen, R. Wahlström, U. Liimatainen, T. Liitiä, S. Rovio, J. K. J. Helminen, U. Hyväkkö, A. W. T. King, A. Suurnäkki and I. Kilpeläinen, Sustainability of cellulose dissolution and regeneration in 1,5-diazabicyclo[4.3.0]non-5-enium acetate: a batch simulation of the IONCELL-F process, *RSC Adv.*, 2015, **5**, 69728–69737.
10 L. K. J. Hauru, M. Hummel, A. W. T. King, I. Kilpeläinen and H. Sixta, Role of solvent parameters in the regeneration of cellulose from ionic liquid solutions, *Biomacromolecules*, 2012, **13**, 2896–2905.
11 N. L. Mai, K. Ahn and Y.-M. Koo, Methods for recovery of ionic liquids—a review, *Process Biochemistry*, 2014, **49**, 872–881.
12 J. Palomar, J. Lemus, M. A. Gilarranz and J. J. Rodriguez, Adsorption of ionic liquids from aqueous effluents by activated carbon, *Carbon*, 2009, **47**, 1846–1856.
13 D. C. Dibble, C. Li, L. Sun, A. George, A. Cheng, Ö. P. Çetinkol, P. Benke, B. M. Holmes, S. Singh and B. A. Simmons, A facile method for the recovery of ionic liquid and lignin from biomass pretreatment, *Green Chem.*, 2011, **13**, 3255–3264.
14 T. Rosenau, A. Potthast, H. Sixta and P. Kosma, The chemistry of side reactions and byproduct formation in the system NMMO/cellulose (Lyocell process), *Progress in Polymer Science*, 2001, **26**, 1763–1837.
15 A. W. T. King, J. Asikkala, I. Mutikainen, P. Järvi and I. Kilpeläinen, Distillable acid–base conjugate ionic liquids for cellulose dissolution and processing, *Angewandte Chemie International Edition*, 2011, **50**, 6301–6305.
16 K. Massonne, M. Siemer, W. Mormann and W. Leng, *Distillation of ionic liquids*, Google Patents, 2013.
17 A. Ostonen, J. Bervas, P. Uusi-Kyyny, V. Alopaeus, D. H. Zaitsau, V. N. Emel'yanenko, C. Schick, A. W. T. King, J. Helminen, I. Kilpeläinen, A. A. Khachatrian, M. A. Varfolomeev and S. P. Verevkin, Experimental and Theoretical Thermodynamic Study of Distillable Ionic Liquid 1,5-Diazabicyclo[4.3.0]non-5-enium Acetate, *Ind. Eng. Chem. Res.*, 2016, **55**, 10445–10454.
18 A. W. T. King, A. Parviainen, P. Karhunen, J. Matikainen, L. K. J. Hauru, H. Sixta and I. Kilpeläinen, Relative and inherent reactivities of imidazolium-based ionic liquids: the implications for lignocellulose processing applications, *RSC Adv.*, 2012, **2**, 8020–8026.
19 T. Schäfer, C. M. Rodrigues, C. Am Afonso and J. G. Crespo, Selective recovery of solutes from ionic liquids by pervaporation—a novel approach for purification and green processing, *Chemical Communications*, 2001, 1622–1623.
20 J. Sun, J. Shi, Murthy Konda, N. V. S. N., D. Campos, D. Liu, S. Nemser, J. Shamshina, T. Dutta, P. Berton, G. Gurau, R. D. Rogers, B. A. Simmons and S. Singh, Efficient dehydration and recovery of ionic liquid after lignocellulosic processing using pervaporation, *Biotechnology for Biofuels*, 2017, **10**, 154.
21 L. Su, M. Li, X. Zhu, Z. Wang, Z. Chen, F. Li, Q. Zhou and S. Hong, In situ crystallization of low-melting ionic liquid [BMIM][PF6] under high pressure up to 2 GPa, *The Journal of Physical Chemistry B*, 2010, **114**, 5061–5065.
22 A. R. Choudhury, N. Winterton, A. Steiner, A. I. Cooper and K. A. Johnson, In situ crystallization of low-melting ionic liquids, *Journal of the American Chemical Society*, 2005, **127**, 16792–16793.
23 N. Osmanbegovic, L. Yuan, H. Lorenz and M. Louhi-Kultanen, Freeze Concentration of Aqueous [DBNH][OAc] Ionic Liquid Solution, *Crystals*, 2020, **10**, 147.
24 A. Michud, M. Tanttu, S. Asaadi, Y. Ma, E. Netti, P. Kääriainen, A. Persson, A. Berntsson, M. Hummel and H. Sixta, Ioncell-F: ionic liquid-based cellulosic textile fibers as an alternative to viscose and Lyocell, *Textile Research Journal*, 2016, **86**, 543–552.
25 M. Hummel, A. Michud, M. Tanttu, S. Asaadi, Y. Ma, L. K. J. Hauru, A. Parviainen, A. W. T. King, I. Kilpeläinen and H. Sixta, in *Cellulose Chemistry and Properties: Fibers, Nanocelluloses and Advanced Materials*, Springer, 2015, pp. 133–168.
26 M. J. Kamlet and R. W. Taft, The solvatochromic comparison method. I. The beta.-scale of solvent hydrogen-bond acceptor (HBA) basicities, *Journal of the American Chemical Society*, 1976, **98**, 377–383.
27 R. W. Taft, J.-L. M. Abboud and M. J. Kamlet, Solvatochromic comparison method. 20. Linear solvation energy relationships. 12. The d.delta. term in the solvatochromic equations, *Journal of the American Chemical Society*, 1981, **103**, 1080–1086.
28 W. Ahmad, A. Ostonen, K. Jakobsson, P. Uusi-Kyyny, V. Alopaeus, U. Hyväkkö and A. W.T. King, Feasibility of thermal separation in recycling of the distillable ionic liquid [DBNH][OAc] in cellulose fiber production, *Chemical Engineering Research and Design*, 2016, **114**, 287–298.
29 F. M. S. Ribeiro, C. F. R. A. C. Lima, I. C. M. Vaz, Rodrigues, Ana S. M. C., E. Sapei, A. Melo, A. M. S. Silva and L. M. N. B. F. Santos, Vaporization of protic ionic liquids derived from organic superbases and short carboxylic acids, *Phys. Chem. Chem. Phys.*, 2017, **19**, 16693–16701.
30 F. M. S. Ribeiro, C. F. R. A. C. Lima, A. M. S. Silva and L. M. N. B. F. Santos, Experimental Evidence for Azeotrope Formation from Protic Ionic Liquids, *Chemphyschem : a European journal of chemical physics and physical chemistry*, 2018, **19**, 2364–2369.
31 2018.
32 A. M. Hyde, R. Calabria, R. Arvary, X. Wang and A. Klapars, Investigating the Underappreciated Hydrolytic Instability of 1,8-Diazabicyclo[5.4.0]undec-7-ene and Related Unsaturated Nitrogenous Bases, *Org. Process Res. Dev.*, 2019, **23**, 1860–1871.
33 A. Potthast, T. Rosenau, R. Buchner, T. Röder, G. Ebner, H. Bruglachner, H. Sixta and P. Kosma, The cellulose solvent system N, N-dimethylacetamide/lithium chloride revisited: the effect of water on physicochemical properties and chemical stability, *Cellulose*, 2002, **9**, 41–53.
34 A. Potthast, S. Radosta, B. Saake, S. Lebioda, T. Heinze, U. Henniges, A. Isogai, A. Koschella, P. Kosma and T. Rosenau, Comparison testing of methods for gel permeation chromatography of cellulose: coming closer to a standard protocol, *Cellulose*, 2015, **22**, 1591–1613.
35 L. Jürgen, S. Josef and W. E., *On the Elongation Mechanism of Regenerated Cellulose Fibres*, 2009, vol. 48, **48,** https://www.degruyter.com/view/j/hfsg.1994.48.issue-

s1/hfsg.1994.48.s1.72/hfsg.1994.48.s1.72.xml.

36 Z. S. Baird, A. Dahlberg, P. Uusi-Kyyny, N. Osmanbegovic, J. Witos, J. Helminen, D. Cederkrantz, P. Hyväri, V. Alopaeus, I. Kilpeläinen, S. K. Wiedmer and H. Sixta, Physical Properties of 7-Methyl-1,5,7-triazabicyclo[4.4.0]dec-5-ene (mTBD), *Int J Thermophys*, 2019, **40**, 1607.

37 H. Turkia, H. Sirén, J.-P. Pitkänen, M. Wiebe and M. Penttilä, Capillary electrophoresis for the monitoring of carboxylic acid production by Gluconobacter oxydans, *Journal of Chromatography A*, 2010, **1217**, 1537–1542.

38 M. Lechuga, M. Fernández-Serrano, E. Jurado, J. Núñez-Olea and F. Ríos, Acute toxicity of anionic and non-ionic surfactants to aquatic organisms, *Ecotoxicology and Environmental Safety*, 2016, **125**, 1–8.

39 B. Viard, C. Guizani and H. Sixta, Master's dissertation, Aalto University, 2019.

40 M. Mori, N. Rath, C. Gobble, J. Chickos, A. A. Samarov and S. P. Verevkin, Vaporization, Sublimation Enthalpy, and Crystal Structures of Imidazo[1,2-a]pyrazine and Phthalazine, *Journal of Chemical & Engineering Data*, 2016, **61**, 370–379.

41 I. Kaljurand, A. Kütt, L. Sooväli, T. Rodima, V. Mäemets, I. Leito and I. A. Koppel, Extension of the Self-Consistent Spectrophotometric Basicity Scale in Acetonitrile to a Full Span of 28 pKa Units: Unification of Different Basicity Scales, *The Journal of Organic Chemistry*, 2005, **70**, 1019–1028.

42 K. T. Leffek, P. Pruszynski and K. Thanapaalasingham, Basicity of substituted 2-phenyl-1,1,3,3- tetramethylguanidines and other bases in acetonitrile solvent, *Can. J. Chem.*, 1989, **67**, 590–595.

43 K. Huang, R. Wu, Y. Cao, H. Li and J. Wang, Recycling and Reuse of Ionic Liquid in Homogeneous Cellulose Acetylation, *Chinese Journal of Chemical Engineering*, 2013, **21**, 577–584.

44 S. ‐ K. Ruokonen, C. Sanwald, A. Robciuc, S. Hietala, A. H. Rantamäki, J. Witos, A. W. T. King, M. Lämmerhofer and S. K. Wiedmer, Correlation between ionic liquid cytotoxicity and liposome‐ionic liquid interactions, *Chemistry–A European Journal*, 2018, **24**, 2669–2680.

45 H.-P. Fink, P. Weigel, H. J. Purz and J. Ganster, Structure formation of regenerated cellulose materials from NMMO-solutions, *Progress in Polymer Science*, 2001, **26**, 1473–1524.

46 T. Röder, J. Moosbauer, K. Wöss, S. Schlader and G. Kraft, Man-made cellulose fibres–a comparison based on morphology and mechanical properties, *Lenzinger Berichte*, 2013, **91**, 7–12.

Supporting information

Recycling of Superbase-Based Ionic Liquid Solvents for the Production of Textile-Grade Regenerated Cellulose Fibers in the Lyocell Process

Sherif Elsayed,[a] Sanna Hellsten,[a] Chamseddine Guizani,[a] Joanna Witos,[a] Marja Rissanen,[a] Antti H. Rantamäki,[b] Pauliina Varis,[c] Susanne K. Wiedmer[b] and Herbert Sixta*[a]

[a] Department of Bioproducts and Biosystems, Aalto University, P.O. Box 16300, FI-00076 Aalto, Finland.

[b] Department of Chemistry, University of Helsinki, P.O. Box 55, FI-00014 University of Helsinki, Helsinki, Finland.

[c] Marimekko Corporation, P.O. Box 107, 00811 Helsinki, Finland.

E-mail: sherif.elsayed@aalto.fi, sanna.hellsten@aalto.fi, chamseddine.guizani@aalto.fi, Joanna.witos@aalto.fi, marja.rissanen@aalto.fi, herbert.sixta@aalto.fi, antti.rantamaki@helsinki.fi, susanne.wiedmer@helsinki.fi, pauliina.varis@marimekko.com

Contents

Number of pages: 08
Number of tables: 05
Number of figures: 02

Hydrolysis pathways

The mechanism of the hydrolysis reactions commence via the reaction of water with the unsaturated nitrogenous group in [DBNH][OAc] producing 1-(3-aminopropyl)-2-pyrrolidonium acetate ([APPH][OAc]), and in [mTBDH][OAc] producing 1-[3-(methyl ammonio)propyl]-1,3-diazinan-2-onium ([H-mTBD-1][OAc]), (H-mTBD-1) and 1-(3-ammoniopropyl)-3-methyl-1,3-diazinan-2-onium ([H-mTBD-2][OAc]), as illustrated in Figure S1.

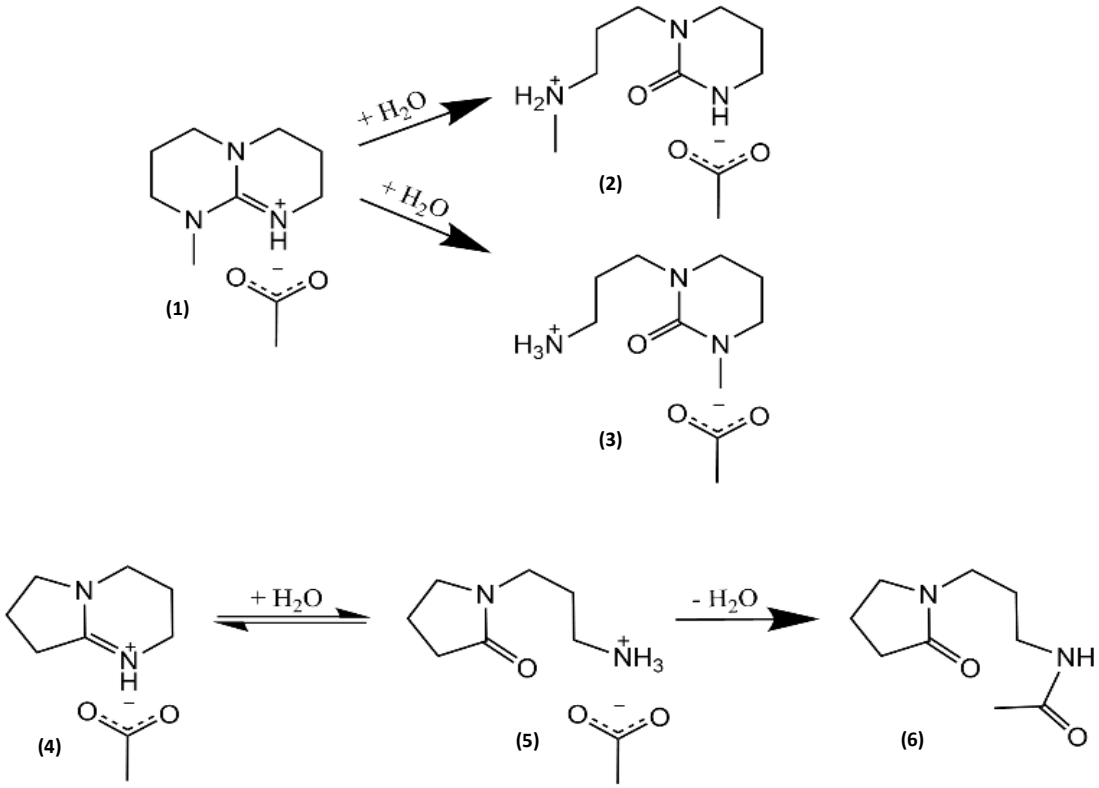

Figure S1 Hydrolysis of [mTBDH][OAc] (1) into [H-mTBD-1][OAc] (2) and [H-mTBD-2][OAc] (3) and hydrolysis of [DBNH][OAc] (4) into [APPH][OAc] (5) and condensation into APPAc (6).

Capillary electrophoresis

In brief, the calibration curves were acquired for mTBD, DBN, and their degradation products at a concentration range of 0.01 mg·mL^{-1} to 0.2 mg·mL^{-1}. Benzyltrimethylammonium chloride (Sigma Aldrich, Steinheim, Germany) with 0.02 mg/mL concentration was used as an internal standard. The CE separation was as follows: voltage - 25 kV (mTBD and its degradation products), - 20 kV (DBN and its degradation products), sample injection 10 s at 10 mbar, temperature of the cassette and the autosampler 25 °C, and UV detection at 200 nm. The background electrolyte (BGE) solution was composed of sodium acetate buffer at pH 4.0 with the ionic strength of 10 mM and 20 mM for DBN and its decomposition products, and likewise, for mTBD and its decomposition products. The pH of the BGE solutions was adjusted to the

desired value with 1M sodium hydroxide or 1 M hydrochloric acid. Before use, the BGE solution was filtered through a 0.45 µm PVDF filters (Phenomenex, Denmark).

The acetate concentration was determined following a modified capillary zone electrophoresis method to the above-mentioned protocol. The CE experiments were performed with a Hewlett Packard 3D CE model G1600GX (Agilent, Waldbronn, Germany). The acetate calibration curve was comprised of nine acetic acid solutions with concentrations between 0.0025 mg/mL and 0.2 mg/mL. Propionic acid (Acrõs Organics/Thermo Fischer Scientific, Geel, Belgium) with a 0.05 mg/mL concentration was used as an internal standard. The correlation coefficient of the calibration curve was 0.9997. The BGE solution was composed of 20 mM 2,3-pyridinedicarboxylic acid (Sigma-Aldrich, Steinheim, Germany) and 0.3 mM myristyltrimethylammonium hydroxide (100 mM concentrate, Waters, Milford, USA) in 10:90 (v/v) MeOH:H_2O. The pH of the solution was adjusted to 9 with 25% (v/v) ammonia (VWR international, Leuven, Belgium). The buffer was filtered through a 0.45 µm PVDF filter (Aireka Cells, Wan Chai, Hong Kong) before use. The sample was injected hydrodynamically at 45 mbar for 10 s. The separation was performed using a voltage of - 10 kV at 25 °C and the indirect UV detection was done by a diode-array UV-Vis detector at 254 nm.

Dress making

Spin and yarn finishing

The fibers spun from fresh and recovered [mTBD][OAc] dopes were spin finished with a mixture of Afilan CVS:Leomin PN (80:20) (Archroma, Switzerland). The spin finish concentration in the bath was 0.83 g/L and the liquor-to-dry fiber ratio was 20:1. The treatment proceeded at 50 ºC for 5 min. Following the treatment, the fibers were pressed to a final amount of spin finish of 0.25% before air-drying. Next, using a fiber opener (Trash Analyzer 281C Mesdan Lab, Mesdan S.p.A. Italy), the dried fibers were opened and conditioned over night at 20°C and 65% relative humidity prior to yarn spinning.
The fibers were carded (Carding Machine 337A, Mesdan Lab, Mesdan S.p.A., Italy) in batches of 25 g to obtain a fiber web, which was formed manually into a sliver. Each sliver was elongated with a draw frame (Stiro Roving Lab 3371, Mesdan Lab, Mesdan S.p.A, Italy), doubled with another sliver and elongated again. After drafting, the sliver was doubled, drawn, and false-twisted to form a roving. The yarn spinning proceeded with a ring spinning machine (Ring Lab 82BA, SER.MA.TES Srl, Italy). The target count of yarn was 20 tex (Nm 50/1, Ne 30/1) employing a Z direction twist and incorporated 900 twists per meter with a twist factor (αe) of 4.2.

Yarn tensile testing

Tenacity and elongation at break of the spun yarn was determined by MTS 400 tensile tester equipped with 50 N load cell using a gauge length of 250 mm, a test speed of 250 mm/min, and a specimen number of 30. Before measuring, the yarn was conditioned overnight (20 ± 2 °C and 65 ± 2 % relative humidity) and the average linear density value was evaluated from a 10 m hank of yarn (n=14). As a reference Tencel™ yarn tensile testing, the commercial

Tencel™ yarn (20 tex, Nm 50/1, Ne 30/1) was provided by Orneule Oy, Finland. The determined twist per meter was 880 and the torsion was Z.

Weaving and printing

The yarn (20 tex Z 900) was used as a filling yarn (weft yarn) in the weaving machine (Picanol, Belgium) in the weaving mill (Söktaş Tekstil A.Ş, Turkey). The warp yarn was commercial Tencel™ -yarn (Nm 50/1, Ne 30/1) with a density of 48 yarns/cm and a weft of 29 yarns/cm. The weave structure was twill. The fabric width was 150 cm and the mass per unit area was 139 g/m2. The calculated share of Tencel™ was 62 wt.% and the Ioncell® share 38%. After the weaving the fabric was pre-treated to remove the impurities from the fabric and to improve the absorption of dyes in the subsequent printing. The fabric was pre-treated in the same factory where it was weaved, and the pre-treatment processes were similar to those used for the lyocell-type fabrics. First, the protruding fibers were removed by the singeing process and the warp sizes were removed in the desizing process. Then it was washed to remove the dirt. Cold mercerization (NaOH 20º Bé) improved the dye uptake (Goswami *et al*. 2011). The cellulase enzyme wash cleaned the fabric surface (Morgado *et al*. 2000; Carrillo *et al*. 2003). Finally, the fabric was dried and transported to the printing mill.
The fabric was printed in the Marimekko Oy printing mill (Finland). The navy-blue reactive dye (Huntsman Novacron® P) was printed onto the fabric with a rotary-screen printing machine. The print design was "Unikko" designed by Maija Isola in 1964. The dye was fixed in a steamer with 103 °C saturated steam for 8 min. The reactive dye print recipe was similar to the one that the company uses for cotton fabric printing. The amount of used urea was 100 g/kg. After fixation, the fabric was washed at 95 °C to remove unfixed dye and printing paste auxiliaries. Finally, the printed fabric was dried at room temperature. After the printing, the fabric was finished in the same factory as where it was weaved. The fabric finishing gives the final visual appearance and functionality to the fabric. The fabric was resin finished (resin + low density polyethylene resin (LDPE) + MicroSilicone + wetting agent, no acid) to improve the wrinkle recovery (Jaturapiree *et al*. 2011). Pentek finishing is a mechanical finishing which give a soft touch to the fabric. The sanforiing process reduces the shrinkage of the fabric (Ahn *et al*. 2005).

Dress making

The dress was sewn in the Marimekko factory in Finland. The interlining fabric was attached to the fabric (collar, cuffs, belt, and front pieces) by ironing with steam at 141 ºC for 12 s. The edge text for the dress was transfer printed with phthalate and heavy metal free opaque plastisol ink (Texiplast 7000) on the transfer print paper. The edge text was attached by ironing with steam at 160 °C for 15 s on the fabric (included glue).
Fabric testing. The color fastness to washing (EN ISO 105-C06) at 30ºC and 40ºC, to rubbing (EN ISO X-12), and to alkaline and acid perspiration (EN ISO 105-E04) were tested. The Martindale-equipment was used for the determination of pilling (EN ISO 12945-2) and abrasion resistance (EN ISO 12947-2). The tensile strength of fabric was determined according to the grab-test (EN ISO 13934-2). The tearing strength was determined using Elmendorf equipment (ISO 13937-1). The resistance to the seam slippage was determined by the fixed

opening method (ISO 13936-1). The dimensional changes were determined after laundering at 30 ºC. The test results were evaluated in comparison to a 100% Tencel™ control fabric with similar weave structure, fabric density and fabric weight. The fabric tests were conducted by Marimekko and Intertek. Table S1 contains comprehensive properties of the blended fabric [mTBDH][OAc] fibers and Tencel™

The breaking force and the breaking tenacity of the Ioncell® yarn are higher than the Tencel™ yarn, Table S2, implying a higher total chain orientation of the former fibers. Meanwhile, the standard deviation of Ioncell® yarn is somehow large, which means that the evenness of the yarn fibers is slightly less. This is due to the small-scale production and the absence of auto-levelling possibility in the Ioncell® yarn production process.

Table S1 The fabric testing results of the Tencel/Ioncell blend fabric (62/38 wt.%) and a reference, 100% Tencel fabric. Color fastness and pilling ratings are from 1 to 5 where 5 is the best rating.

Property		**Ioncell/Tencel fabric**	**Tencel fabric***
Dimensional change after 30 ºC washing (%)	Warp	+2.2	+1.8
	Weft	+2.6	+0.4
Color fastness to washing at 30 ºC	Shade change	4	Blue 4 White 3-4
	Staining CO	4	4
Color fastness to washing at 40 ºC	Shade change	4-5	4
	Staining CO	4	4
Color fastness to rubbing after laundering at 30 ºC	Dry	4-5	3
	Wet	3-4	3
Color fastness to perspiration	Shade change	4-5	n.a.
	Staining CO	4-5	n.a.
Tensile strength (N)	Warp	495	n.a.
	Weft	127	n.a.
Tear strength (g)	Warp	1946	n.a.
	Weft	1880	n.a.
Pilling		4-5	4-5
Abrasion resistance (cycles)		2000	4000
Seam slippage (N)	Warp	116	n.a.
	Weft	>200	n.a.

*Tencel fabric as a reference.

Table S2 Yarn mechanical properties for Marimekko demonstration dress.

Yarn	Linear density	Breaking force	Elongation at break	Breaking tenacity
	tex	cN	%	cN/tex
[mTBDH][OAc] - Ioncell®	19.9 ± 0.9	490 ± 77	5.7 ± 0.7	24.6 ± 3.7
Tencel™	19.9 ± 0.2	443 ± 34	7.7 ± 0.7	22.3 ± 1.7

IL recovery

Table S3 shows the composition of the distillate and residue streams in the centrifuge evaporator and TFE-1. The amount of H-mTBD in the distillate and concentrate from the centrifuge evaporator were well below the detection limit, probably due to the mild conditions of the centrifugal bath (62 °C and 250 mbar) and the high IL dilution in the feed and the concentrate. For the same reasons, very little traces of hydrolysis products (< 0.06 wt.%) were detected in the distillate of TFE-1 (61 °C and 20 mbar) with no presence in the concentrate.

Table S3 Distillate and residue compositions of the centrifuge evaporator and the TFE-1.

Cycle	Centrifuge evaporator				TFE-1			
	Distillate		Residue		Distillate		Residue	
	[mTBD][OAc]	H-mTBD	[mTBD][OAc]	H-mTBD	[mTBD][OAc]	H-mTBD	[mTBD][OAc]	Acid/mTBD
	wt.%	wt.%	wt.%	wt.%	wt.%	wt.%	wt.%	mole ratio
1	0.14 ± 0.01	-	45.6 ± 1.5	-	0.03 ± 0.01	-	84.1 ± 0.8	1.02
2	0.14 ± 0.01	-	23.1 ± 0.7	-	0.05 ± 0.01	0.004 ± 0.001	84.9 ± 0.03	1.02
3	0.07 ± 0.01	-	6.3 ± 0.5	-	0.03 ± 0.01	-	70.4 ± 1.2	1.05
4	0.09 ± 0.01	-	9.2 ± 0.4	-	0.23 ± 0.01	0.065 ± 0.002	72.9 ± 0.8	1.12
5	0.10 ± 0.01	-	7.2 ± 0.7	-	0.03 ± 0.01	-	60.4 ± 3.2	1.11

Toxicity assay

Toxicity values measured with vibrio ficscheri bacteria for the amide products produced through the irreversible condensation reactions of the hydrolysis products. From APPH, the condensation reaction yields the 1-(3-acetamidopropyl)-2-pyrrolidone (APPAc), and 1-[3-(acetamido)propyl]-1,3dyiazinan-2-one (A-mTBD) from H-mTBD.

Table S4 Toxicities of amides from [DBNH][OAc] and [mTBDH][OAc].

Compound	*Vibrio fischeri*			
	5 min		**15 min**	
	mg/L	mM	mg/L	mM
APPAc	2024 ± 213	11 ± 1.2	2191 ± 138	11.9 ± 1
A-mTBD	2851 ± 288	13.4 ± 1.4	3378 ± 363	15.8 ± 1.7

Rheology

The zero-shear viscosities (η_0) of the [DBNH][OAc] and [mTBDH][OAc] dopes are directly compared in Figure S2. It is clear that the latter possess a higher complex viscosity for all measured temperature points. This suggests a higher temperature needed during spinning in order to adjust a η_0.

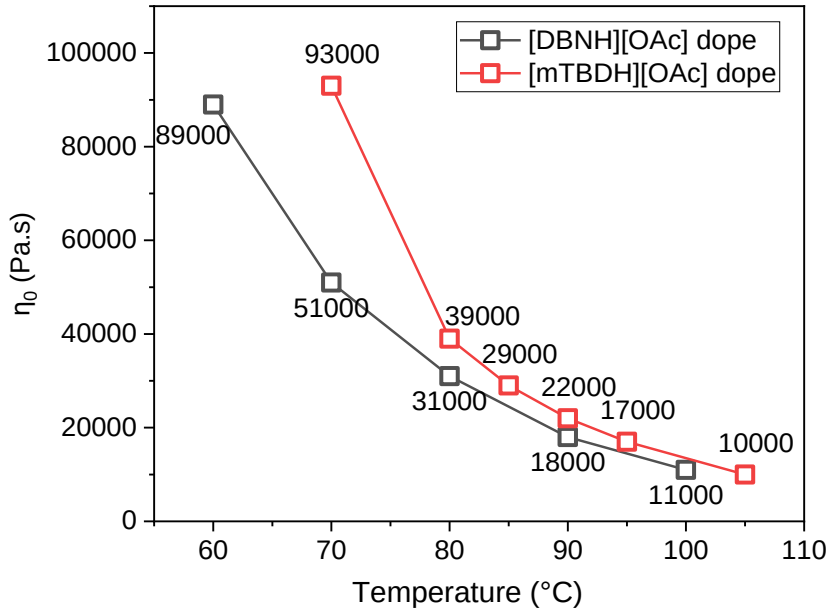

Figure S2 η_0 of fresh [mTBDH][OAc]dope vs fresh [DBNH][OAc] dope.

Kamlet-Taft parameters

N,N-diehyl-4-nitro-aniline (DENA, Sigma), 4-nitroaniline (NA, Sigma), and 2,6-dichloro-(2,4,6-triphenyl-1-pyridino) phenolate (WB, prepared in the lab according to Kessler and Wolfbeis 1989) were dissolved in acetone to yield 30 mmol solutions, respectively. 10 µl DENA, 30 µl NA, and 100 - 500 µl WB were then transferred to separate Eppendorf tubes, which were left open until all the acetone was evaporated leaving behind solid dye residues. Afterwards, 500 µl of IL was added to the tubes. The mixtures were heated in an oven (100°C, 5 min) and subsequently vortexed to dissolve the dyes in the IL. The IL solutions were transferred to glass cuvettes using a syringe of appropriate dimensions. To determine the Kamlet-Taft parameters, the UV spectra of these solutions were recorded (Shimadzu UV-2550 spectrophotometer) between 200 - 600 nm and their peak maxima λ (λ_{DENA} = 402 - 414 nm, λ_{NA} = 398 - 406 nm, λ_{WB} = 518 - 585 nm were calculated via Gaussian or polynomial fit functions. λ was then inserted in the equations below to obtain the solvent polarity values

(ET(30) and ET(33)), the di-polarity polarizability ratio (π*), the hydrogen bond acidity (α), and the hydrogen bond basicity (β) as descriptors of the solubility of cellulose in ionic liquid solutions.

$$ET(30) = 0.979 * ET(33) - 7.461 \quad \text{(S1)}$$

$$ET(33) = \frac{28591.5}{\lambda_{WB}} \quad \text{(S2)}$$

$$\pi^* = 0.314 * \left(27.52 - \frac{1}{\lambda_{DENA} * 0.0001}\right) \quad \text{(S3)}$$

$$\alpha = 0.0649 * ET(30) - 2.03 - (0.72 * \pi^*) \quad \text{(S4)}$$

$$\beta = \left(1.035 * \frac{1}{\lambda_{DENA} * 0.0001} + 2.64 - \frac{1}{\lambda_{NA} * 0.0001}\right) * 2.8^{-1} \quad \text{(S5)}$$

Table S5 Kamlet-Taft parameters of [DBNH][OAc]and [mTBDH][OAc].

IL	ET(33) kcal/mol	ET(30) kcal/mol	π*	α	β	β-α
[DBNH][OAc]	58.92	50.12	0.96	0.53	1.10	0.57
[mTBDH][OAc]	57.63	48.96	1.01	0.42	1.17	0.75

References

Ahn, C.; Yoo, H.J.; Oh, Y.S.; Han, S.S.; Lee, H.J.; Kim, J.H.; Song, K.H.; Rhie, J.S. Evaluating the physical and fabric hand characteristics of lyocell fabrics made with different wood pulps. *Textile research journal* **2005**, 75(2), 139–143, DOI 10.1177/004051750507500209.

Carrillo, F.; Colom, X.; Valldeperas, J.; Evans, D.; Huson, M.; Church, J. Structural characterization and properties of lyocell fibres after fibrillation and enzymatic defibrillation finishing treatments. In *Textile Research Journal* **2003***,* 73 (11), 1024–1030, DOI10.1177/004051750307301114.

Goswami, P.; Blackburn, R.S.; Taylor, J.; White, P. Sorption of dyes on cellulose II: effect of alkali treatment of fibre and dye structure. *Cellulose* **2011**, 18(4), 1063–1072, DOI 10.1007/s10570-011-9540-0.

Jaturapiree, A.; Manian, A.P.; Lenninger, M.; Bechtold, T. The influence of alkali pretreatments in lyocell resin finishing—Changes in fiber accessibility to crosslinker and catalyst. *Carbohydrate polymers* **2011**, 86(2), 612–620, DOI 10.1016/j.carbpol.2011.04.085.

Morgado, J.; Cavaco-Paulo, A.; Rousselle, M.A. Enzymatic treatment of lyocell—clarification of depilling mechanisms. *Textile Research Journal* **2000**, 70(8), 696–699, DOI 10.1177/004051750007000807.

Kessler, M.A.; Wolfbeis, O.S. ET (33), a solvatochromic polarity and micellar probe for neutral aqueous solutions. *Chemistry and physics of lipids* **1989**, 50(1), 51–56, DOI 10.1016/0009-3084(89)90025-X.